MICROPHONE SQUEAL AND MACHINING CHATTER

Tony L. Schmitz
Department of Mechanical Engineering and Engineering Science
University of North Carolina at Charlotte
Charlotte, NC, USA

INTRODUCTION

Self-excited vibration, or regenerative chatter, in machining has been studied for many years. The research topic has encouraged the application of mathematics, dynamics (linear and nonlinear), controls, heat transfer, tribology, and other disciplines to the field of machining science. In particular, a foundational understanding of regenerative chatter was established by the application of the Nyquist criterion from controls theory to the feedback system generated by machining processes [1]. The purpose of this paper is to demonstrate the analogy between the squeal frequency experienced when audio feedback causes instability in public address systems [2] and the chatter frequency exhibited by machining operations. A simple microphone/speaker setup is described and experimental results are quantitatively and qualitatively compared to machining stability predictions.

MACHINING STABILITY MODEL

To describe the linear stability analysis, turning is considered here. However, the approach may be extended to milling and other machining processes. When a flexible tool is used to cut away material in the form of a chip, the corresponding cutting force causes time-dependent deflections of the cutting tool. As the vibrating tool removes material, these vibrations are imprinted on the workpiece surface as a wavy profile. Figure 1 depicts an exaggerated view, where the initial impact with the workpiece surface causes the tool to begin vibrating and the oscillations in the normal direction to be copied onto the workpiece [3]. When the workpiece begins its second revolution, the vibrating tool encounters the wavy surface produced during the first revolution. Subsequently, the chip thickness at any instant depends both on the tool deflection at that time and the workpiece surface from the previous revolution. Vibration of the tool causes a variable chip thickness in the sensitive direction, y, which yields a variable cutting force since the force is proportional to the chip thickness. See Eq. 1, where F is the cutting force, K_s is the specific cutting force, b is the chip width, h_m is the mean chip thickness, $y(t-\tau)$ is the vibration in the previous revolution, y is the current vibration, and τ is the time delay (i.e., the time for one revolution). The force is separated into the mean, F_m, and variable, F_v, components. Because the cutting force governs the current tool deflection through the structural dynamics, the system exhibits feedback.

$$F = K_s b\left(h_m + y(t-\tau) - y\right) = K_s b h_m + K_s b\left(y(t-\tau) - y\right) = F_m + F_v \quad (1)$$

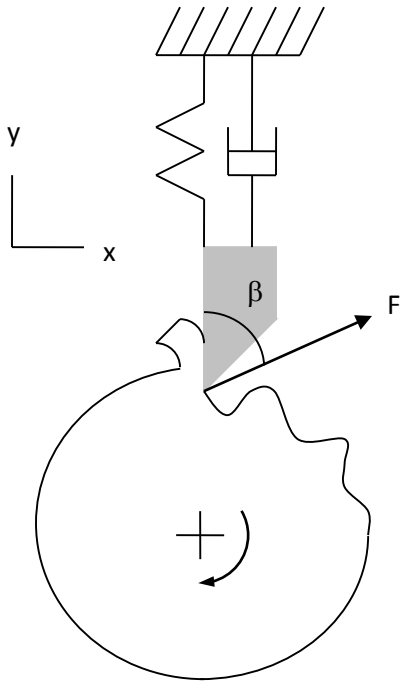

Figure 1: A flexible tool deflects due to the cutting force [3]. These deflections are imprinted on the workpiece surface and cause a variable chip thickness in the next revolution.

Equation 1 can be expressed as a block diagram as shown in Fig. 2. The y-direction projection of the variable force component (through the force angle, β) excites the structural dynamics in the y-

direction. The dynamics are described using the frequency response function, or FRF, in that direction. The time-delayed deflection, $y(t-\tau)$, is represented using the exponential function, where $\varepsilon = \tau\omega$ is the phase (in rad) between current and previous tool vibrations and ω is the frequency (rad/s).

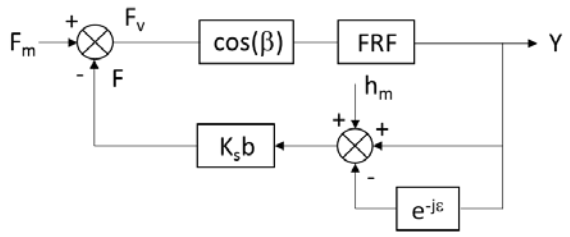

Figure 2: Block diagram description of the turning process [1]. The variable component of the cutting force excites the structure's FRF after projection into the y-direction. The corresponding frequency domain vibration, Y, is summed with the vibration from the previous revolution and mean chip thickness, and finally scaled by the product of the specific cutting force and chip width to produce the cutting force.

The Nyquist criterion is applied to Fig. 2 to identify the limit of stability, where the chip width, b, acts as the system gain. The limiting chip width, b_{lim}, is obtained when the open loop transfer function is set equal to -1 as shown in Eq. 2.

$$K_s b_{lim} FRF\left(1 - e^{-j\varepsilon}\right) = -1 \qquad (2)$$

Equation 2 can be rewritten to relate b_{lim} to the real (Re) part of the FRF as shown in Eq. 3. Additional relationships for the phase and spindle speed are provided in Eqs. 4 and 5 [3].

$$b_{lim} = \frac{-1}{2K_s \cos(\beta) Re[FRF]} \qquad (3)$$

$$\frac{f_c}{\Omega} = N + \frac{\varepsilon}{2\pi} \qquad (4)$$

$$\varepsilon = 2\pi - 2\tan^{-1}\left(\frac{Re[FRF]}{Im[FRF]}\right) \qquad (5)$$

In Eq. 4, f_c is the chatter frequency (should it occur), Ω is the spindle speed, N is the integer number of waves of vibration imprinted on the workpiece surface in one revolution, and $\frac{\varepsilon}{2\pi}$ is any additional fraction of a wave. Note that for units consistency in Eq. 4, if f_c is expressed in Hz, then Ω must be specified in rev/s.

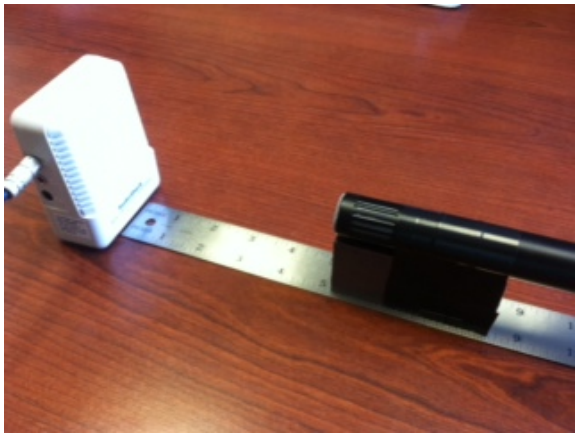

Figure 3: Experimental setup. The speaker is on the left and the unidirectional microphone is on the right. The distance between them is determined using the steel scale.

EXPERIMENTAL SETUP

In public address systems when a microphone/speaker combination is used to amplify the microphone input, a similar feedback phenomenon is observed. In this case, the speaker output can re-enter the microphone after some delay defined by the time for the sound to travel from the speaker to the microphone. This generates a time-delay feedback system analogous to the machining case. An experimental setup is constructed to explore the system instability, which is exhibited as an audible squeal frequency, and demonstrate its similarity to the chatter frequency in machining.

The setup is pictured in Fig. 3, where a Radioshack Mini Amplifier/Speaker and a Switchcraft unidirectional microphone are aligned and the distance between them is varied. The distance is observed using a steel scale. The speaker volume can also adjusted to modify the system gain. The speaker volume is the analog to chip width in machining.

RESULTS

Measurements were performed to identify: 1) the system natural frequency(s); and 2) the squeal frequency, f_s, as a function of the distance between the speaker and microphone, d. The natural frequencies were determined by

introducing a known audio frequency into the microphone, measuring the speaker output, and then incrementing the frequency over the range of interest. The Fourier transform of both signals was then calculated and the ratio of the speaker output magnitude to the microphone input magnitude at the test frequency was determined (this is the sine sweep approach used in traditional modal testing). This result is displayed in Fig. 4; a modal fit is also included, where second order dynamics were assumed. Although other fits could be considered, only two clear peaks (near 2000 Hz and 4000 Hz) were evident and it was believed that the other points were near the noise floor of the measurements. The modal parameters for the two-mode fit are provided in Table 1. For these measurements, the Tone Generator application [4] for the iPhone was used as the frequency source and the Voice Memos application (in the iPhone utilities menu for a second iPhone) was used to record the speaker output (44.1 kHz sampling rate with no additional digital filtering). The .m4a sound files were then analyzed in Matlab®.

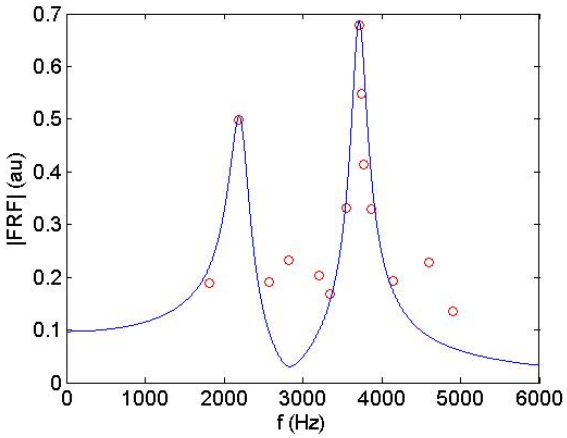

Figure 4: Ratio of the speaker output magnitude to the microphone input magnitude in arbitrary units, au (circles). A modal fit (solid line) is also shown.

Table 1: Parameters for modal fit to microphone/speaker FRF magnitude.

Mode	Natural freq. (Hz)	Stiffness (au)	Viscous damping ratio
1	2215	17	0.06
2	3713	26.2	0.028

The modal parameters in Table 1 were used to approximately represent the system dynamics as a frequency response function, FRF, and the stability limit and squeal frequency were predicted using Eqs. 3-5. The time delay, τ, was first calculated as the inverse of the predicted spindle speed vector from Eq. 4. The time delay was then related to the distance between the speaker and microphone using Eq. 6, where v is the velocity of sound in dry air at 20 deg C (343 m/s).

$$d = v\tau \qquad (6)$$

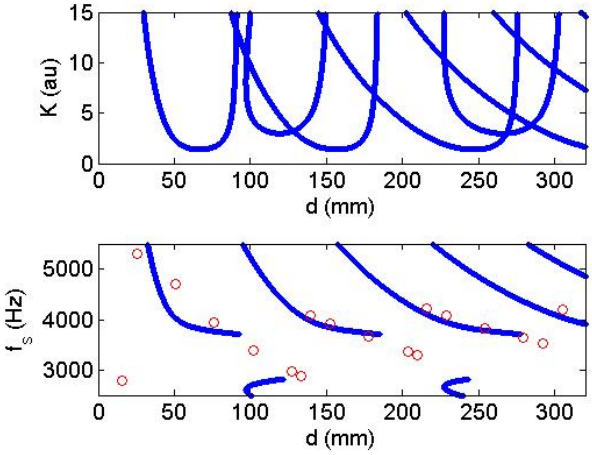

Figure 5: (Top) Stability prediction as a function of distance between the speaker and microphone, d, and the audio system gain, K (arbitrary units, au). The solid lines indicate the stability boundaries (unstable above). (Bottom) Squeal frequency, f_s, prediction as a function of d (solid line). Experimental results are shown as open circles.

Figure 5 (top panel) shows the stability limit as a function of the gain, K, and distance. Any {d, K} combination above the stability boundaries is predicted to be unstable (i.e., squeal occurs). The vertical axis gain is the chip width in machining, but depends on the speaker volume and acoustic cavity (the volume surrounding the speaker and microphone) for the public address system. Because the FRF test results displayed in Fig. 4 were obtained with the speaker and microphone separated (to separate the source and response measurements), they do not include the inherent acoustic cavity effects. Therefore, the gain units are not provided and only qualitative comparisons between the speaker volume (gain) and stability can be completed; when applying Eq. 3, the product $K_s \cos(\beta)$ was assumed to be unity.

Figure 5 (bottom panel) shows the chatter frequency as a function of the distance between the speaker and microphone. In this case, the squeal frequency could be measured using the

Voice Memos application so a direct comparison is possible. The chatter frequency prediction from the machining stability analysis is shown as the solid line, while the squeal frequency measurements are plotted as circles.

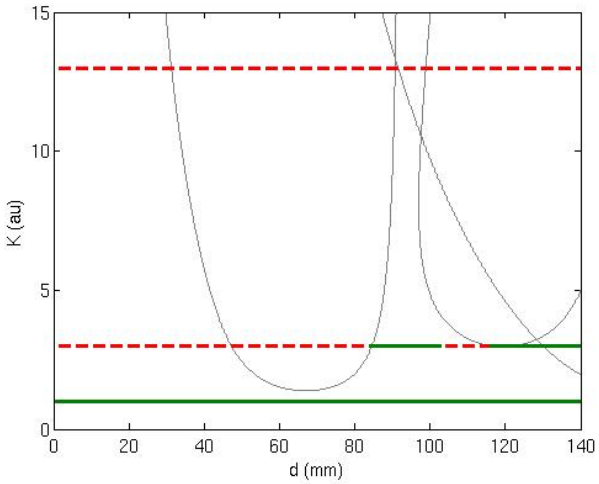

Figure 6: Stability comparison at three speaker volume (gain) values. The highest gain (top line) exhibited squeal at all locations. The dotted line indicates squeal/instability. This gain provided the squeal frequencies for Figure 5. A lower volume produced squeal only at particular distances (middle line). Stable (no squeal) distances are identified by the solid line. Below a threshold volume value, no squeal occurs (bottom line).

The squeal frequency results in Fig. 5 show good quantitative agreement with the machining analysis chatter frequencies in all cases except for the smallest distance between the speaker and microphone (d = 15.9 mm point). It is proposed that this unstable result is due to acoustic cavity affects and is outside the scope of this study. To provide a qualitative stability comparison, the speaker volume was varied from high to low and the regions of squeal (unstable) and no squeal (stable) were recorded. The results for three volume, or gain, values are presented in Fig. 6. Because the cavity gain was not measured, the vertical locations of the three gains (i.e., the horizontal lines in Fig. 6) were selected to approximately match the stability boundary in Fig. 6. This is equivalent to applying the machining stability predictions to a system where K_s and β are unknown. In this case it is possible to identify preferred spindle speeds (horizontal axis), but not limiting depths of cut (vertical axis). Qualitative assessment of stability is possible, but vertical scaling of the chip width is not.

While the bottom panel of Fig. 5 provides clear evidence that the squeal frequency produced by time-delay feedback in the speaker/microphone setup provides an analogy to the chatter frequency in machining, a more compelling expression of the behavior is established by audio/video from a continuous scan of the distance between the speaker and microphone. It is seen and heard that the squeal frequency periodically rises and falls as the distance is varied; the video is available online [5].

In addition, video is provided that shows both a forward (microphone moving toward the speaker) and reverse direction sweep [5]. As displayed in Fig. 8, it is observed that the dramatic shifts in squeal frequency (bifurcations) do not occur at the same spatial locations between the two directions. This indicates nonlinear behavior.

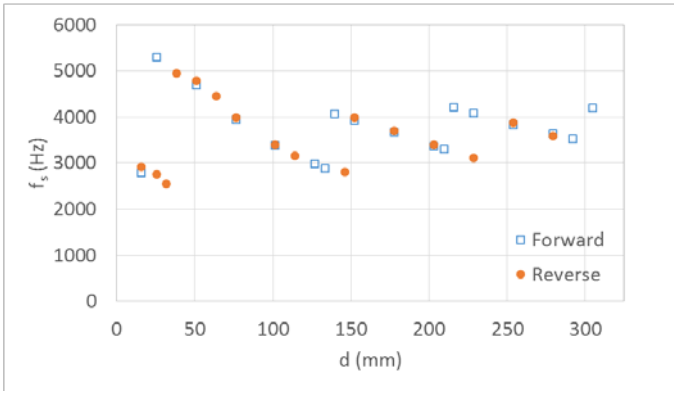

Figure 7: A discrepancy between the shifts in squeal frequency with distance is observed between the forward and reverse paths.

CONCLUSIONS

It was demonstrated that a direct analogy exists between audio feedback in public address systems and chatter in machining; both are time-delay feedback systems with stability that depends on the system gain.

REFERENCES

[1] Tlusty J (2000) Manufacturing Processes and Equipment. Prentice Hall, Upper Saddle River, NJ, pp. 568-570.

[2] Schroeder MR (1964) Improvement of acoustic-feedback stability by frequency shifting, The Journal of the Acoustic Society of America, 36/9:1718-1724.

[3] Schmitz T, Smith S (2009) Machining Dynamics: Frequency Response to Improved Productivity. Springer, New York, NY.

[4] http://www.lifegrit.com.

[5] http://coefs.uncc.edu/tschmit4/videos/.